Journal of the Franklin Institute, Available online 20 July 2020
DOI: 10.1016/j.jfranklin.2020.07.022

Sliding Mode Control of a Class of Underactuated System With Non-integrable Momentum

Lejun Chen[a,*], Mien Van[b]

[a]*School of Aerospace, Transport and Manufacturing, Cranfield University, U.K.*
[b]*School of Electronics, Electrical Engineering and Computer Science, Queen's University Belfast, U.K.*

Abstract

In this paper, a sliding mode control scheme is developed to stabilise a class of nonlinear perturbed underactuated system with a non-integral momentum. In this scheme, by initially maintaining a subset of actuated variables on sliding manifolds, the underactuated system with the non-integrable momentum can be approximated by one with the integrable momentum in finite time. During sliding, a subset of the actuated variables converge to zero and a physically meaningful diffeomorphism is systematically calculated to transform the reduced order sliding motion into one in a strict feedback normal form in which the control signals are decoupled from the underactuated subsystem. Furthermore, based on the perturbed strict feedback form, it is possible to find a sliding mode control law to ensure the asymptotic stability of the remaining actuated and unactuated variables. The design efficacy is verified via a multi-link planar robot case study.

Keywords: Sliding mode control, Underactuated System, Robotics.

1. Introduction

In recent decades there has been increasing interest in Euler-Lagrange systems (Spong et al., 2004; Dong & Chen, 2019). Underactauted Euler-Lagrange systems, which have fewer independent actuation inputs than the number of degrees of freedom (DOF) or configuration variables, have received

*Corresponding author.
Email addresses: Lejun.Chen@cranfield.ac.uk (Lejun Chen), M.Van@qub.ac.uk (Mien Van)

extensively attentions in a broad range of applications including robotic and aerospace systems. For example, crane systems (Cheng & Chen, 1996; Fang et al., 2012; Lu et al., 2018b), Pendubot (Shoji et al., 2013; Shah & Rehman, 2018), Acrabot (Spong, 1996), surface vessel (Hu et al., 2016; Ghommam & Mnif, 2009; Wang et al., 2019), hypersonic vehicles (Wang et al., 2017), quadrotor systems (Zhao et al., 2015; Zou & Meng, 2019) and flexible or multi-link manipulators (Chen & Shan, 2020; Lai et al., 2017; Wang et al., 2020; Yan et al., 2019). Although underactuated systems has a lower number of actuators compared with one associated with overactuated systems, the complexity of the control system design is increased. A state-of-the-art overview of the modelling, classification, control and application of the underactuated system can be found in Olfati-Saber (2001).

Sliding mode control schemes have several unique properties, and these have sustained research interest in this area since the 1960s. The most important property is its insensitivity (at least theoretically) to matched uncertainty acting in the control input channels (Utkin, 1992; Edwards & Spurgeon, 1998; Shtessel et al., 2013). In conventional sliding mode systems, the order of the closed-loop system is reduced compared to the open-loop, by an amount equal to the number of input control signals. The reduced order dynamics during the sliding motion are determined by the choice of sliding surface – which is a key component of the design process. Many different approaches for the design of linear sliding surfaces for uncertain linear systems have been developed, and the area is quite mature (Edwards & Spurgeon, 1998; Shtessel et al., 2013). In conventional sliding modes the closed-loop behaviour has two quite distinguishable phases: a) the pre-sliding phase in which the system states are driven towards the sliding surface to create a sliding mode; b) the reduced order sliding motion that occurs once the surface is attained. As a promising method, sliding mode control schemes have been used to stabilise Euler-Lagrange systems (Van et al., 2019; Jiang et al., 2018) and underactuated systems (Olfati-Saber, 2002; Park et al., 2006; Ashrafiuon & Erwin, 2008; Nersesov et al., 2014). Specifically, in Olfati-Saber (2002), a cascade normal form has been introduced to facilitate the design of controllers for underactuated system. In Nersesov et al. (2014), a general framework based on sliding mode control has been developed to provide an asymptotic stabilization of uncertain underactuated nonlinear systems. Some recent works have successfully stabilised underactuated systems in the face of the external disturbances (Xu & Özgüner, 2008; Lu et al., 2018a; Huang et al., 2019; Du et al., 2019), modelling uncertainty (Roy & Baldi, 2020;

Do & Lee, 2020) or even faults/failures (Chen & Shan, 2020). Specifically, in Xu & Özgüner (2008), an underactuated system was firstly transformed to a cascade form, and then a sliding mode controller has been designed to stabilizing the indirectly controlled modes. In Lu et al. (2018a), a similar diffeomorphism as in Xu & Özgüner (2008) was developed to transform the underactuated system into a cascade form, and a continuous second order sliding mode controller is then developed. An integration between sliding mode control and disturbance observer has been developed in Huang et al. (2019) to eliminate the external disturbances. In Do & Lee (2020), a back-stepping sliding mode control has been developed for an underactuated system based on an neural network approximation. The recent work in Roy & Baldi (2020) released structure-specific constraints in the Euler Lagrange system using an adaptive scheme. In scheme developed in Do & Lee (2020) considered input constraints as well as matched and mismatched uncertainties and the influence of actuator saturation is also examined via an auxiliary system.

To control underactuated systems, some works systematically developed a global change of coordinate which is capable of transforming an underactuated system with symmetry into one in a strict feedback normal form (Olfati-Saber, 2000). The main advantages of using this class of global coordinate transformation are: a) the order of the underactuated system can be reduced; b) some conventional control design and controllability analysis approaches, such like sliding mode control, back-stepping control and adaptive control, can be applied to a system in the normal form straightforwardly; c) the control inputs are decoupled from the unactuated variables, which reduces the complexity of the control system design. As argued in Olfati-Saber (2001), the key analytical tools which allow reduction of high-order underactuated systems using a global change of coordinate in explicit forms are normalized generalized momentums and their integrals. The integrability of theses normalized momentums plays a fundamental role in the structure of the normal forms for high-order underactuated systems and an important property of normal forms for high-order underactuated systems is that they are physically meaningful. The global change of coordinate can be obtained from the Lagrangian of the system and the reduced order system is a well-defined reduced Lagrangian system that satisfies the Euler-Lagrange equations. Many works in the literature (e.g in Olfati-Saber (2002, 2000); Xu & Özgüner (2008); Huang et al. (2019); Lu et al. (2018a); Shah & Rehman (2018)) assumed that the normalised momentum conjugated to

the unactuated variables is integrable. However, some high-order underactuated systems do not possess integrable normalized momentums such as the flexible robot and 3D Cart-Pole system. For an underactuated system with the non-integrable momentum, the global change of coordinate is not straightforwardly applicable because the shape inertial matrix is not exact one (Olfati-Saber, 2000). In Olfati-Saber (2001), a methodology, so called decomposition momentum, was used to decompose the normalised momentum into an integrable locked momentum and a non-integrable error momentum. However, the diffeomorphism or a global change of coordinate, used to approximate the locked momentum, contains a large computational load, especially for a high order system.

The main contribution of this paper is to stabilise a class of perturbed underactuated systems with the non-integrable momentum based upon using a sliding mode control approach. Instead of using momentum decomposition proposed in Olfati-Saber (2001), the non-integrable normalised momentum can be approximated by an integrable momentum, via maintaining a subset of the actuated variables on sliding manifolds. During sliding, a subset of actuated variables approach to zero in finite time and a physically meaningful diffeomorphism, which has the capability of transforming the reduced order sliding motion into one in the strict feedback normal form, is systematically calculated. This paper also shows that the scheme may guarantee the asymptotic stability of both actuated and unactuated variables despite external disturbances.

The remainder of the paper is structured as follows: some preliminaries are in given in Section 2; in Section 3 the sliding mode control scheme, which ensures the possible asymptotic stability of both actuated and unactuated variables, is discussed. The simulation results, associated with a multi-link planar robot, are presented in Section 4. Finally, Section 5 provides some concluding remarks.

The notation used in this paper is quite standard: in particular, the norm of a vector $x \in \mathbb{R}^n$ is defined as $\|x\| = \sqrt{x^T x}$ and the norm of a matrix $A \in \mathbb{R}^{n \times n}$ is given by $\|A\| = \sqrt{\delta_{max}(A^T A)}$ where $\delta_{max}(A^T A)$ represents the maximum eigenvalue of $A^T A$. For $A \in \mathbb{R}^{m \times n}$, the pseudo inverse of A is denoted by $A^\dagger \in \mathbb{R}^{n \times m}$.

2. Preliminary

Consider a nonlinear underactuated Euler-Lagrange system

$$M(q_a)\ddot{q} + W(q,\dot{q})\dot{q} + F(q,\dot{q}) = Bu + d \tag{1}$$

where

$$B = \begin{bmatrix} I_{n-m} \\ 0_{m\times(n-m)} \end{bmatrix} \tag{2}$$

and $u \in \mathbb{R}^{n-m}$ denotes the system inputs. In (1), $M(q_a) \in \mathbb{R}^{n\times n}$ represents the inertial matrix, $W(q,\dot{q}) \in \mathbb{R}^{n\times n}$ captures the the Coriolis and centrifugal forces, and $F(q,\dot{q}) \in \mathbb{R}^n$ represents the damping and friction terms. In (1), the variable $q = [q_a^T \;\; q_u^T]^T$ denotes system state variables, where $q_a \in \mathbb{R}^{n-m}$ represents the actuated variables and $q_u \in \mathbb{R}^m$ denotes the unactuated variables. The signal d is used to capture the external disturbance, and it is assumed that $d = [d_a^T \;\; d_u^T]^T$ where $d_a \in \mathbb{R}^{n-m}$ and $d_u \in \mathbb{R}^m$ represent the disturbances affecting the actuated and unactuated channels, respectively. In this paper, it is assumed that $\|d\| \leq \xi$.

Suppose $M(q_a)$ in (1) has the following structure

$$M(q_a) = \begin{bmatrix} M_{11}(q_a) & M_{12}(q_a) \\ M_{21}(q_a) & M_{22}(q_a) \end{bmatrix} \tag{3}$$

where $M_{11}(q_a) \in \mathbb{R}^{(n-m)\times(n-m)}$ and $M_{22}(q_a) \in \mathbb{R}^{m\times m}$. In (1), $W(q,\dot{q})$ and $F(q,\dot{q})$ are given by

$$W(q,\dot{q}) = \begin{bmatrix} W_1(q,\dot{q}) \\ W_2(q,\dot{q}) \end{bmatrix}, \quad F(q,\dot{q}) = \begin{bmatrix} F_1(q,\dot{q}) \\ F_2(q,\dot{q}) \end{bmatrix} \tag{4}$$

where $W_2(q,\dot{q}) \in \mathbb{R}^{m\times n}$ and $F_2(q,\dot{q}) \in \mathbb{R}^m$. Define

$$N(q,\dot{q}) := W(q,\dot{q})\dot{q} + F(q,\dot{q}) \tag{5}$$

and suppose $N(q,\dot{q})$ has the structure

$$N(q,\dot{q}) = \begin{bmatrix} N_1(q,\dot{q}) \\ N_2(q,\dot{q}) \end{bmatrix} \tag{6}$$

where $N_1(q,\dot{q}) \in \mathbb{R}^{n-m}$ and $N_2(q,\dot{q}) \in \mathbb{R}^m$.

Notice that the system in (1) is with symmetry, i.e. the inertial matrix only corresponds to the actuated variables q_a.

Assumption 2.1. *It is assumed that $n - m \leq m < n$, which is a realistic assumption for most of Euler-Lagrange systems (e.g. in Cheng & Chen (1996); Fang et al. (2012); Lu et al. (2018b); Shoji et al. (2013); Shah & Rehman (2018); Spong (1996); Zhao et al. (2015)).*

Property 2.1. *As argued in Spong et al. (2004), for most of Euler-Lagrange systems, $M(q_a)$ is a symmetric and uniformly positive definite matrix which satisfies*

$$0 < c_1 I_n \leq M(q_a) \leq c_2 I_n \tag{7}$$

Assumption 2.2. *In this paper, it is assumed that the equilibrium points are zero.*

Remark 2.1. *Without loss of generality, by applying a suitable coordinate transformation, any known fixed equilibrium points can be shifted to zero.*

From equations (1)-(4) and the definition in (5) and (6), it follows

$$\ddot{q}_u = -M_{22}^{-1}(q_a)(M_{21}(q_a)\ddot{q}_a + N_2(q, \dot{q}) - d_u) \tag{8}$$

Define

$$M_a(q_a) = M_{11}(q_a) - M_{12}(q_a)M_{22}^{-1}(q_a)M_{21}(q_a) \tag{9}$$

and substitute (8) into (1) yields

$$M_a(q_a)\ddot{q}_a - M_{12}(q_a)M_{22}^{-1}(q_a)(N_2(q, \dot{q}) - d_u) + N_1(q, \dot{q}) = u + d_a \tag{10}$$

Now define a collocated partial linearisation law as

$$u = M_a(q_a)v + N_1(q, \dot{q}) - M_{12}(q_a)M_{22}^{-1}(q_a)N_2(q, \dot{q}) \tag{11}$$

where $v \in \mathbb{R}^{n-m}$ represents the virtual control input to be calculated.

Remark 2.2. *From (7) it follows that $M_a^{-1}(q_a)$ always exists. Furthermore $M_{11}(q_a)$ and $M_{22}(q_a)$ are bounded and symmetric positive definite (s.p.d) since $M(q_a)$ is s.p.d.*

Now substituting the control law in (11) into (1), the Euler-Lagrange system in (1) can be written in the form of

$$\begin{aligned} \ddot{q}_u &= -M_{22}^{-1}(q_a)M_{21}(q_a)v - M_{22}^{-1}(q_a)N_2 + \sigma(\cdot) \\ \ddot{q}_a &= v + M_a^{-1}(q_a)(d_a - M_{12}(q_a)M_{22}^{-1}(q_a)d_u) \end{aligned} \tag{12}$$

where the perturbed term $\sigma(\cdot)$ is given by

$$\sigma(\cdot) = -M_{22}^{-1}(q_a)M_{21}(q_a)M_a^{-1}(q_a)(d_a - M_{12}(q_a)M_{22}^{-1}(q_a)d_u) + M_{22}^{-1}(q_a)d_u \tag{13}$$

Remark 2.3. *It can be seen from (12) that the virtual control input v affects both the actuated and unactuated variables, which increases the complexity of control design for underactuated systems. In the sequel, a global change of coordinate will be selected to decouple v from the unactuated subsystem.*

Suppose the system in (1) involves the kinetic energy $\mathcal{K}$ and the dissipative energy $\mathcal{D}$, the Lagrangian is

$$\frac{d}{dt}(\frac{\partial \mathcal{K}}{\partial \dot{q}}) - \frac{\partial \mathcal{K}}{\partial q} + \frac{\partial \mathcal{D}}{\partial \dot{q}} = Bu + d \tag{14}$$

where $\mathcal{K} = \frac{1}{2}\dot{q}^T M(q_a)\dot{q}$. In (14), $\mathcal{D} = \frac{1}{2}\dot{q}^T D(q_a)\dot{q}$ where $D(q_a)$ corresponds to the dissipative coefficients, e.g. the coefficients of friction of the translational or rotational motion. Futhermore, it follows $F(q,\dot{q}) = D(q_a)\dot{q}$. The relationship between the Lagrange equation and the equation of motion in (1) is established as

$$\frac{d}{dt}(\frac{\partial \mathcal{K}}{\partial \dot{q}}) - \frac{\partial \mathcal{K}}{\partial q} + \frac{\partial \mathcal{D}}{\partial \dot{q}} = \begin{bmatrix} M_{11}(q_a) & M_{12}(q_a) \\ M_{21}(q_a) & M_{22}(q_a) \end{bmatrix} \begin{bmatrix} \ddot{q}_a \\ \ddot{q}_u \end{bmatrix} + \begin{bmatrix} W_1(q,\dot{q}) \\ W_2(q,\dot{q}) \end{bmatrix} \dot{q} + \begin{bmatrix} F_1(q,\dot{q}) \\ F_2(q,\dot{q}) \end{bmatrix} \tag{15}$$

and the last m equations in (15) associated with q_u are

$$\frac{d}{dt}(\frac{\partial \mathcal{K}}{\partial \dot{q}_u}) - \frac{\partial \mathcal{K}}{\partial q_u} + \frac{\partial \mathcal{D}}{\partial \dot{q}_u} = M_{21}(q_a)\ddot{q}_a + M_{21}(q_a)\ddot{q}_u + W_2(q,\dot{q})\dot{q} + F_2(q,\dot{q}) = d_u \tag{16}$$

where

$$\frac{\partial \mathcal{D}}{\partial \dot{q}_u} = F_2(q,\dot{q}) \tag{17}$$

$$\frac{d}{dt}(\frac{\partial \mathcal{K}}{\partial \dot{q}_u}) = M_{21}(q_a)\ddot{q}_a + M_{22}(q_a)\ddot{q}_u + W_2(q,\dot{q})\dot{q} \tag{18}$$

Since $\mathcal{K} = \frac{1}{2}\dot{q}^T M(q_a)\dot{q}$ is dependent on $\dot{q}_u$ but does not depend on q_u explicitly, it can be obtained that

$$\frac{\partial \mathcal{K}}{\partial \dot{q}_u} = M_{21}(q_a)\dot{q}_a + M_{22}(q_a)\dot{q}_u \tag{19}$$

$$\frac{\partial \mathcal{K}}{\partial q_u} = 0 \tag{20}$$

The above properties in (17)-(20) will be exploited in the sequel.

From (19), the normalized momentum conjugated to q_u can be written as

$$\pi = M_{22}^{-1}(q_a)\frac{\partial \mathcal{K}}{\partial \dot{q}_u} = \dot{q}_u + \underbrace{M_{22}^{-1}(q_a)M_{21}(q_a)}_{\mu(q_a)}\dot{q}_a \tag{21}$$

where $\mu(q_a) \in \mathbb{R}^{m\times(n-m)}$ is referred as the shape inertial matrix. If there exists a generalized configuration function $\delta = \delta(q)$ such that $\dot{\delta}(q,\dot{q}) = \nabla\delta(q)\dot{q} = \pi$, π is an integrable normalized momentum and $\delta(q)$ is referred as the integral of π. If there does not exist a function δ which satisfies $\dot{\delta} = \pi$, π is non-integrable.

Assumption 2.3. *It is assumed that $\mu(q_a)dq_a$ is not exact one form.*

Remark 2.4. *As argued in Olfati-Saber (2001), if $\mu(q_a)dq_a$ is not exact one form, the normalized momentum π in (21) is non-integrable, and the diffeomorphism (e.g. used in Xu & Özgüner (2008); Huang et al. (2019); Lu et al. (2018a)), which is capable of transforming (12) into one in the strict feedback normal form, cannot be calculated systematically.*

Suppose there exists $h \leq m$ and assume q_a is given by

$$q_a = \begin{bmatrix} q_{v1}^T & q_{v2}^T \end{bmatrix}^T \tag{22}$$

where $q_{v1} \in \mathbb{R}^h$ and $q_{v2} \in \mathbb{R}^{n-m-h}$. In the situation when $q_{v2} = 0$, the shape inertial matrix $\mu(q_a)$ in (21) can be written as $\mu(q_{v1}, 0)$ and this quantity will be used in the following assumption.

Assumption 2.4. *Suppose the pair (i, j) satisfies*

$$\frac{\partial \mu_i(q_{v1},0)}{\partial q_{v1,j}} = \frac{\partial \mu_j(q_{v1},0)}{\partial q_{v1,i}} \quad \forall\ i,j = 1,\cdots,h \tag{23}$$

where $\mu_i(q_{v1},0)$ denotes the ith column of $\mu(q_{v1},0)$ in (21) and $q_{v1,i}$ denotes ith component of q_{v1}, and it is also assumed that indices i and j in (23) satisfy the following relationships:

$$\begin{cases} i \neq j & \text{if} \quad m \geq h > 1 \\ i = j = 1 & \text{if} \quad h = 1 \end{cases} \tag{24}$$

Remark 2.5. *Notice that the determination of q_{v1} and q_{v2} is not unique. To check the availability of (23), the components in q_a can be reordered.*

Remark 2.6. *The value h will be used in the following section to select $n-m-h$ actuated variables to be maintained on predefined sliding manifolds.*

3. Control of the underactuated system

In this section, a global change of coordinate in closed form will be derived, via inducing sliding for a subset of actuated variables, to transform (12) into one in the strict feedback form. Then the remaining DOF will be further exploited, based on the strict feedback system, to ensure the asymptotic stability of the left actuated and unactuated variables.

3.1. Global diffeomorphism with non-integrable momentum

Let the virtual control input v in (11) be decomposed into $v = \begin{bmatrix} v_1^T & v_2^T \end{bmatrix}^T$ where $v_1 \in \mathbb{R}^h$ and $v_2 \in \mathbb{R}^{n-m-h}$, then from (12), $\ddot{q}_{v1}$ and $\ddot{q}_{v2}$ can be written as

$$\ddot{q}_{v1} = v_1 + \underbrace{\begin{bmatrix} I_h & 0_{h\times(n-m-h)} \end{bmatrix} M_a^{-1}(q_a)(d_a - M_{12}(q_a)M_{22}^{-1}(q_a)d_u)}_{h_1(\cdot)} \tag{25}$$

$$\ddot{q}_{v2} = v_2 + \underbrace{\begin{bmatrix} 0_{(n-m-h)\times h} & I_{n-m-h} \end{bmatrix} M_a^{-1}(q_a)(d_a - M_{12}(q_a)M_{22}^{-1}(q_a)d_u)}_{h_2(\cdot)} \tag{26}$$

Clearly, from (12), $n-m$ variables q_a are actuated. If the virtual control input $v_2 \in \mathbb{R}^{n-m-h}$ can be selected to ensure that $n-m-h$ actuated variables q_{v2} approaches to zero, only the remaining h actuated variables q_{v1} and m unactuated variables q_u will appear in a reduced order system. In the following part of the section, v_2 will be calculated using a sliding mode based approach.

Define a sliding manifold $s \in \mathbb{R}^{n-m-h}$ as

$$s = \dot{q}_{v2} + \Lambda q_{v2} \tag{27}$$

where $\Lambda \in \mathbb{R}^{(n-m-h)\times(n-m-h)}$ is a positive definite matrix and let $M_{21}(q_a) \in \mathbb{R}^{m\times(n-m)}$ be partitioned as

$$M_{21}(q_a) = \begin{bmatrix} M_{211}(q_a) & M_{212}(q_a) \end{bmatrix} \tag{28}$$

where $M_{211}(q_a) \in \mathbb{R}^{m\times h}$ and $M_{212}(q_a) \in \mathbb{R}^{m\times(n-m-h)}$.

The following theorem shows that a non-integrable momentum can be approximated by an integrable momentum via maintaining $n-m-h$ selected actuated variables at s.

Theorem 3.1. *The virtual control law v_2 is designed as*

$$v_2 = v_{2l} + v_{2n} \tag{29}$$

where the linear part is

$$v_{2l} = -\Lambda \dot{q}_{v2} \tag{30}$$

and the nonlinear part is defined as

$$v_{2n} = -K(t)\frac{s}{\|s\|} \quad \text{for} \quad s \neq 0 \tag{31}$$

In (31) the modulation function $K(t)$ is selected as

$$K(t) = \|M_a^{-1}(q_a)\|(1 + \|M_{12}(q_a)M_{22}^{-1}(q_a)\|)\xi + \eta \tag{32}$$

where η is a positive scalar. By applying v_2 to (12), the non-integrable momentum π in (21) can be approximated by an integrable momentum π_s defined as

$$\pi_s = \dot{q}_u + \underbrace{M_{22}^{-1}(q_{v1})M_{211}(q_{v1})}_{\mu_s(q_{v1},0)}\dot{q}_{v1} \tag{33}$$

in finite time.

Proof. Since by assumption $\|d\| \leq \xi$, both d_a and d_u satisfy

$$\|d_a\| \leq \xi \quad \text{and} \quad \|d_u\| \leq \xi \tag{34}$$

From (27) it follows

$$s^T\dot{s} = s^T(\ddot{q}_{v2} + \Lambda\dot{q}_{v2}) \tag{35}$$

Substituting (26) into (35) and using the definitions in (29)-(31) yields

$$\begin{aligned} s^T\dot{s} &= s^T(v_{2n} + h_2(\cdot)) \\ &\leq -K(t)\|s\| + \|s\|(\|M_a^{-1}(q_a)\|(1 + \|M_{12}(q_a)M_{22}^{-1}(q_a)\|)\xi) \end{aligned} \tag{36}$$

If $K(t)$ is chosen as in (32), then

$$s^T\dot{s} \leq -\eta\|s\| \tag{37}$$

which is a standard reachability condition and sufficient to guarantee that $s = 0$ is maintained (Edwards & Spurgeon, 1998; Utkin, 1992). Integrating (37) implies that the time taken to reach $s = 0$, denoted by t_s, satisfies

$$t_s \leq (0.5\eta)^{-1}\sqrt{s^T(0)s(0)} \tag{38}$$

where $s(0)$ represents the initial value of s at $t = 0$ (Edwards & Spurgeon, 1998). During sliding, $\dot{q}_{v2} \to 0$, $q_{v2} \to 0$, (21) approaches to (33) in finite time. In the situation when $s = 0$, it follows that $\dot{s} = 0$. Hence, s reaches $s = 0$ and cannot escape it, which implies the finite time stability of the origin. From (23), $\mu_s(q_{v1}, 0)dq_{v1}$ is exact one form and the normalized momentum π_s in (21) is integrable (Olfati-Saber, 2001). This completes the proof. □

Since π_s is integrable and the following theorem is proposed to find a global change of coordinate to transform the reduced order sliding dynamic into one in a strict feedback form.

Theorem 3.2. *Define a global change of coordinates as*

$$\begin{aligned} q_r &= q_u + \gamma(q_{v1}) \\ p_r &= M_{22}(q_{v1})(\dot{q}_u + M_{22}^{-1}(q_{v1})M_{211}(q_{v1})\dot{q}_{v1}) \end{aligned} \tag{39}$$

where

$$\gamma(q_{v1}) = \int_0^{q_{v1}} M_{22}^{-1}(\tau)M_{211}(\tau)d\tau \tag{40}$$

and apply it to (12), then (12) can be transformed to one in a strict feedback normal form as

$$\begin{aligned} \dot{q}_r &= M_{22}^{-1}(q_s)p_r \\ \dot{p}_r &= g_r(q_s, q_r, p_s, \dot{q}_r) + d_u \\ \dot{q}_s &= p_s \\ \dot{p}_s &= v_1 + h_1(q_s) \end{aligned} \tag{41}$$

where $h_1(\cdot)$ is defined in (25).

Proof. Since π_s is integrable, calculating the derivative of q_r from (39) yields

$$\dot{q}_r = \dot{q}_u + M_{22}^{-1}(q_{v1})M_{211}(q_{v1})\dot{q}_{v1} \tag{42}$$

Comparing (39) and (42) yields

$$p_r = M_{22}(q_{v1})\dot{q}_r \tag{43}$$

Since during sliding $q_{v2} = 0$, it follows from (42)

$$p_r = M_{22}(q_{v1})\dot{q}_r = M_{22}(q_{v1})\dot{q}_u + M_{211}(q_{v1})\dot{q}_{v1} \tag{44}$$

Using (19) and (22), (44) can be written as

$$p_r = M_{22}(q_a)\dot{q}_u + M_{21}(q_a)\dot{q}_a = \frac{\partial \mathcal{K}}{\partial \dot{q}_u} \tag{45}$$

From (16) and (2) it follows

$$\frac{d}{dt}(\frac{\partial \mathcal{K}}{\partial \dot{q}_u}) - \frac{\partial \mathcal{K}}{\partial q_u} + \frac{\partial \mathcal{D}}{\partial \dot{q}_u} = d_u \tag{46}$$

Consequently the first-order derivative of (45) can be written as

$$\dot{p}_r = \frac{d}{dt}(\frac{\partial \mathcal{K}}{\partial \dot{q}_u}) = \frac{\partial \mathcal{K}}{\partial q_u} - \frac{\partial \mathcal{D}}{\partial \dot{q}_u} + d_u \tag{47}$$

and it follows from (20) that

$$\dot{p}_r = -\frac{\partial \mathcal{D}}{\partial \dot{q}_u} + d_u = g_r(q_a, q_u, \dot{q}_a, \dot{q}_u) + d_u \tag{48}$$

From (39), $q_u = q_r - \gamma(q_{v1})$, $g_r(\cdot)$ in (48) can be written as $g_r(q_{v1}, q_r, \dot{q}_{v1}, \dot{q}_r)$ since $q_{v2} \to 0$ during sliding. After defining $q_s := q_{v1}$ and $p_s := \dot{q}_s$, the proof ends. □

Remark 3.1. *Since the structure property in (23) is exploited, a global change of coordinate is derived without using momentum decomposition (Olfati-Saber, 2001) which requires a complicated coordinate transformation to be found, particularly in terms of high order systems. Furthermore, the momentum decomposition approach may generate an extra perturbed term representing the derivative of the error momentum (Olfati-Saber, 2001).*

3.2. Stabilization of the unactuated variables

As in Xu & Özgüner (2008), a sliding mode based control law will be used to calculate v_1 in (41) such that the remaining actuated variables q_{v1} and unactuated variables q_u will asymptotically converge to the origin.

Define the error variables as

$$\begin{aligned} e_1 &= q_r \\ e_2 &= p_r \\ e_3 &= g_r \\ E &= \begin{bmatrix} e_1 & e_2 \end{bmatrix}^T \end{aligned} \tag{49}$$

where q_r, p_r and g_r are defined in (41). Here, the following assumptions are made:

Assumption 3.1. *The terms $\partial g_r/\partial p_s$ is left invertible, i.e. $\partial g_r/\partial p_s$ has full column rank. As argued in Xu & Özgüner (2008), if $\partial g_r/\partial p_s$ is invertible, then $\|d_u\| < \xi\|E\|$.*

Assumption 3.2. *The terms $\|\partial g_r/\partial p_s\| \leq \beta_1$, $\|\partial g_r/\partial p_r\| \leq \beta_2$ where β_1 and β_2 are positive constants.*

Assumption 3.3. *$g_r(q_s, 0, p_s, 0) = 0$ is an asymptotically stable manifold, i.e., q_s and p_s will converge to 0 if $gr(q_s, 0, p_s, 0) = 0$.*

Remark 3.2. *From Assumption 2.3, $m \geq h$. Then it is possible that $\partial g_r/\partial p_s$ is left invertible and it follows*

$$(\frac{\partial g_r}{\partial p_s})^\dagger = \left((\frac{\partial g_r}{\partial p_s})^T (\frac{\partial g_r}{\partial p_s}) \right)^{-1} (\frac{\partial g_r}{\partial p_s})^T \tag{50}$$

Remark 3.3. *In the case Assumption 3.3 is not satisfactory, it is possible to rewrite d_u as $d_u = d_{u1}(\cdot) + d_{u2}(q_s, 0, p_s, 0)$ where d_{u2} represents the design freedom that allows $g_r(q_s, 0, p_s, 0) + d_{u2}(q_s, 0, p_s, 0) = 0$ to be an asymptotically stable manifold.*

Define a sliding manifold as

$$\Phi = \Psi_1 e_1 + \Psi_2 e_2 + e_3 \tag{51}$$

where $\Psi_1 \in \mathbb{R}^{m\times m}$ and $\Psi_2 \in \mathbb{R}^{m\times m}$ are positive definite matrices which guarantee the following matrix $A_n(q_{v1}) \in \mathbb{R}^{2m\times 2m}$ is Hurwitz.

$$A_n(q_{v1}) := \begin{bmatrix} 0 & M_{22}^{-1}(q_{v1}) \\ -\Psi_1 & -\Psi_2 \end{bmatrix} \tag{52}$$

Lemma 3.1. *According to Property 2.1, it is assumed that*

$$\beta_1 I_m \leq M_{22}^{-1}(q_{v1}) \leq \beta_2 I_m \tag{53}$$

If Ψ_1 *and* Ψ_2 *satisfied the following inequalities*

$$2\lambda_{min}(\Psi_1) + \frac{\beta_1}{\beta_2}\lambda_{min}(\Psi_2) - \lambda_{max}(\Psi_2) - (\lambda_{min}(\Psi_1) + \beta_2)\frac{\lambda_{max}(\Psi_1)}{\lambda_{min}(\Psi_2)} > 0 \tag{54}$$

the matrix $A_n(q_{v1})$ *in (52) is guaranteed to be Hurwitz.*

Proof. Define an Lyapunov matrix as

$$\mathcal{P} = \begin{bmatrix} \alpha_1 I & I_m \\ I_m & \alpha_2 I \end{bmatrix} \tag{55}$$

where the positive scalars α_1 and α_2 are defined as

$$\alpha_1 = \frac{\lambda_{min}(\Psi_2)}{\beta_2} \quad \text{and} \quad \alpha_2 = \frac{\beta_2}{\lambda_{min}(\Psi_2)}(\frac{\lambda_{min}(\Psi_1)}{\beta_2} + 1) \tag{56}$$

and it is easy to verify from (56) that $\alpha_1\alpha_2 > 1$. Now define

$$\mathcal{Q}(q_{v1}) = -(\mathcal{P}A_n(q_{v1}) + A_n^T(q_{v1})\mathcal{P}) \tag{57}$$

and suppose $\mathcal{Q}(q_{v1}) > 0$ has the following structure

$$\begin{aligned} \mathcal{Q}(q_{v1}) &= \begin{bmatrix} \mathcal{Q}_{11} & \mathcal{Q}_{12}(q_{v1}) \\ \mathcal{Q}_{12}^T(q_{v1}) & \mathcal{Q}_{22}(q_{v1}) \end{bmatrix} \\ &= \begin{bmatrix} \Psi_1 + \Psi_1^T & -\alpha_1 M_{22}^{-1}(q_{v1}) + \Psi_2 + \alpha_2\Psi_1^T \\ -\alpha_1 M_{22}^{-1}(q_{v1}) + \Psi_2^T + \alpha_2\Psi_1 & -2M_{22}^{-1}(q_{v1}) + \alpha_2\Psi_2^T + \alpha_2\Psi_2 \end{bmatrix} \end{aligned} \tag{58}$$

Let q_{11} and q_{22} represent the lower bounds of $\mathcal{Q}_{11}$ and $\mathcal{Q}_{22}(q_{v1})$, respectively, and they can be defined as

$$\begin{aligned} q_{11} &= 2\lambda_{min}(\Psi_1) \\ q_{22} &= -2\beta_2 + 2\alpha_2\lambda_{min}(\Psi_2) \end{aligned} \tag{59}$$

Substituting the definition of α_2 in (56) into (59), it can be obtained that

$$q_{11} = q_{22} = 2\lambda_{min}(\Psi_1) \tag{60}$$

Let q_{12} represent the upper bound of $\mathcal{Q}_{12}(q_{v1})$ defined in (58)

$$q_{12} = -\alpha_1\beta_1 + \lambda_{max}(\Psi_2) + \alpha_2\lambda_{max}(\Psi_1) \tag{61}$$

Using (59) and (61) it follows

$$q_{11} - q_{12} = 2\lambda_{min}(\Psi_1) + \alpha_1\beta_1 - \lambda_{max}(\Psi_2) - \alpha_2\lambda_{max}(\Psi_1) \tag{62}$$

Substituting (56) into (62) yields

$$q_{11} - q_{12} = 2\lambda_{min}(\Psi_1) + \frac{\beta_1}{\beta_2}\lambda_{min}(\Psi_2) - \lambda_{max}(\Psi_2) - (\lambda_{min}(\Psi_1) + \beta_2)\frac{\lambda_{max}(\Psi_1)}{\lambda_{min}(\Psi_2)} \tag{63}$$

If (54) is satisfied, $q_{11} - q_{12} > 0$. From (60) it follows $q_{22} - q_{12} > 0$ and therefore it is easy to verify that $\mathcal{Q}(q_{v1}) > 0$. Since $\mathcal{P}$ is proper, from (57) $A_n(q_{v1})$ is Hurwitz. This ends the proof. □

Theorem 3.3. *Let the virtual control law v_1 be*

$$v_1 = v_{1l} + v_{1n} \tag{64}$$

where the components v_{1l} and v_{1n} are defined as

$$\begin{aligned} v_{1l} &= -(\frac{\partial g_r}{\partial p_s})^\dagger((\Psi_1 + \frac{\partial g_r}{\partial q_r})M_{22}^{-1}(q_a)p_r + \Psi_2 g_r + \frac{\partial g_r}{\partial q_s}p_s + \frac{\partial g_r}{\partial p_r}g_r) \\ v_{1n} &= -(\frac{\partial g_r}{\partial p_s})^\dagger(\mathcal{K}(t)\frac{\Phi}{||\Phi||} + \varrho\Phi) \quad \text{for} \quad \Phi \neq 0 \end{aligned} \tag{65}$$

where $(\frac{\partial g_r}{\partial p_s})^\dagger$ is defined in (50), ϱ is a positive scalar to be selected and the modulation function is chosen as

$$\mathcal{K}(t) = \|\Psi_2\|\xi + \beta_2\xi + \beta_1 K(t) + \eta_1 \tag{66}$$

where $K(t)$ is defined in (32). By choosing suitable design parameters Ψ_1 and Ψ_2, all states in (41) asymptotically converge to the origin.

Proof. Define a candidate Lyapunov function as $V = \frac{1}{2}\Phi^T\Phi$, the derivative of V is

$$\begin{aligned} \dot{V} &= \Phi^T\dot{\Phi} = \Phi^T(\Psi_1\dot{e}_1 + \Psi_2\dot{e}_2 + \dot{e}_3) \\ &= \Phi^T(\Psi_1 M_{22}^{-1}(q_s)p_r + \Psi_2 g_r + \Psi_2 d_u + \frac{\partial g_r}{\partial p_s}v_1 + \frac{\partial g_r}{\partial q_s}p_s + \frac{\partial g_r}{\partial q_r}M_{22}^{-1}(q_s)p_r \\ &\quad + \frac{\partial g_r}{\partial p_r}g_r + \frac{\partial g_r}{\partial p_r}d_u + \frac{\partial g_r}{\partial p_s}h_1) \end{aligned} \tag{67}$$

Substituting (65) into (67) yields

$$\begin{aligned}\dot{V} &= \Phi^T(\Psi_2 d_u + \frac{\partial g_r}{\partial p_r}d_u + \frac{\partial g_r}{\partial p_s}h_1) - \Omega\|\Phi\|^2 - \mathcal{K}\|\Phi\| \\ &\leq \|\Phi\|(\|\Psi_2\|\|d_u\| + \|\frac{\partial g_r}{\partial p_r}\|\|d_u\| + \|\frac{\partial g_r}{\partial p_s}\|\|h_1\|) - \varrho\|\Phi\|^2 - \mathcal{K}\|\Phi\|\end{aligned} \tag{68}$$

Using the fact that $\|d_u\| \leq \xi$ and

$$\begin{aligned}\|h_1\| &\leq \|M_a^{-1}(q_a)\|(1 + \|M_{12}(q_a)M_{22}^{-1}(q_a)\|)d_u \\ &\leq \|M_a^{-1}(q_a)\|(1 + \|M_{12}(q_a)M_{22}^{-1}(q_a)\|)\xi < K\end{aligned} \tag{69}$$

Inequality (68) satisfies

$$\dot{V} < \|\Phi\|(\|\Psi_2\|\xi + \|\frac{\partial g_r}{\partial p_r}\|\xi + \|\frac{\partial g_r}{\partial p_s}\|K) - \varrho\|\Phi\|^2 - \mathcal{K}\|\Phi\| \tag{70}$$

From Assumption 3.2,

$$\dot{V} < \|\Phi\|(\|\Psi_2\|\xi + \beta_2\xi + \beta_1 K) - \varrho\|\Phi\|^2 - \mathcal{K}\|\Phi\| \tag{71}$$

Substituting (66) into (71), it follows

$$\dot{V} < -\varrho\|\Phi\|^2 - \eta_1\|\Phi\| \tag{72}$$

Clearly from (72), $\Phi \to 0$ and sliding occurs in finite time. During sliding

$$e_3 = -\Psi_1 e_1 - \Psi_2 e_2 \tag{73}$$

and it follows from (41), (49) and (73) that

$$\dot{e}_2 = e_3 + d_u = -\Psi_1 e_1 - \Psi_2 e_2 + d_u \tag{74}$$

According to the definition of A_n in (52)

$$\dot{E} = A_n E + D \tag{75}$$

where

$$D = \begin{bmatrix} 0 \\ d_u \end{bmatrix} \in \mathbb{R}^{2m\times 1} \tag{76}$$

Next define s.p.d matrices $P \in \mathbb{R}^{2m\times 2m}$ and $Q(q_{v1}) \in \mathbb{R}^{2m\times 2m}$ which satisfy

$$A_n^T(q_{v1})P + PA_n(q_{v1}) = -Q(q_{v1}) \tag{77}$$

and

$$\xi < \frac{\lambda_{\min}(Q(q_{v1}))}{2\lambda_{\max}(P)} \tag{78}$$

Now consider another candidate Lyapunov equation according to $V_1 = E^T P E$, the derivative of V_1 is

$$\dot{V}_1 = \dot{E}^T P E + E^T P \dot{E} \tag{79}$$

Substituting (75) into (79) yields

$$\begin{aligned} \dot{V}_1 &= (E^T A_n^T + D^T) P E + E^T P (A_n E + D) \\ &= E^T (A_n^T P + P A_n) E + 2 E^T P D \\ &\leq -\lambda_{\min}(Q) \|E\|^2 + 2\lambda_{\max}(P) \xi \|E\|^2 \end{aligned} \tag{80}$$

Since $\xi < \lambda_{\min}(Q)/2\lambda_{\max}(P)$, $\dot{V}_1 < 0$ and the origin is asymptotically stable i.e. $e_1 \to 0$ and $e_2 \to 0$. Furthermore, during sliding $\Phi = 0$, $e_3 = g_r = -\Psi_1 e_1 - \Psi_2 e_2 = 0$. From Assumption 3.3, q_s and p_s converge to zero. This completes the proof. □

Remark 3.4. *If Assumption 3.3 is not satisfactory, after a certain period,* $\|E\| \leq 2\|P\|\xi/\lambda_{\min}(Q)$ *and* e_1*,* e_2 *and* e_3 *will converge to a small ball containing the origin.*

Remark 3.5. *Because (39) is global diffeomorphism, the stabilization of (41) only guarantees the stability of the reduced order sliding motion in which* $\dot{s} = s = 0$*.*

Remark 3.6. *In this paper, the stochastic processes are not taken into account. In the situation when there exists various processes with stochastic abrupt structural changes such as the component failures or the contact forces in unknown environment, the system can be modelled as Markov jump systems. Furthermore, due to the non-synchronization phenomenon between the mode of the system and mode of the controller, the novel asynchronous mode dependent sliding mode surface can be used to ensure the finite time stability of the asynchronous stochastic hybrid model (Li et al., 2019; Du et al., 2020).*

4. A six-link robot case study

In this paper a planar multi-link robot is used to evaluate the efficacy of the scheme. The structure of the robot is shown in Fig. 1. Here it is assumed that the robot has six links, i.e. $n = 6$ and is influenced and driven by the ground frictions due to the velocities of the links.

In Fig. 1, θ_i denotes the angle between the ith link and the global x-axis. The length of the link is $2l$ and the variable $\phi_i = \theta_{i+1} - \theta_i,\ \forall\ i = 1, \cdots, 5$ represents the relative angle of ith joint. The torque acting on the ith joint is denoted by $u_i, \forall i = 1, \cdots, 5$. The middle point of the ith link is denoted by (x_i, y_i). It is assumed that the weight and moment of inertia of each link are denoted by $\tilde{m}$ and $J = 1/3\tilde{m}l^2$, respectively. The constants c_t and c_n represent the tangential viscous friction coefficient and the normal viscous friction coefficient, respectively. This model contains six configuration variables $q = \begin{bmatrix} q_a^T & q_u^T \end{bmatrix}^T$ and

$$q_a = \begin{bmatrix} \phi_1, \ldots, \phi_5 \end{bmatrix}^T \quad \text{and} \quad q_u = \theta_6 \tag{81}$$

where q_a denotes five actuated relative joint angles and θ_6 captures one unactuated heading angle.

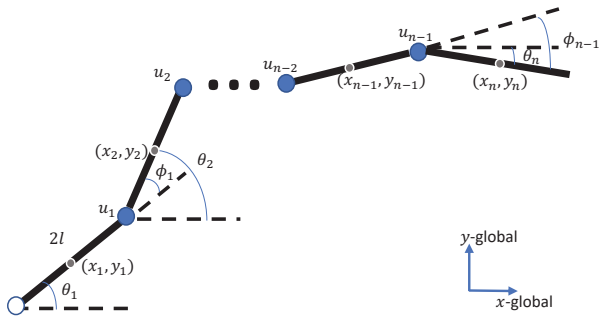

Figure 1: A n-link robot

For the ith link, the force balance equation is given by

$$\tilde{m}\ddot{x}_i = f_{x,i} + \varepsilon_{x,i} - \varepsilon_{x,i-1} \tag{82}$$

$$\tilde{m}\ddot{y}_i = f_{y,i} + \varepsilon_{y,i} - \varepsilon_{y,i-1} \tag{83}$$

where $f_{x,i}$ and $f_{y,i}$ (i.e. the ith component of f_x and f_y) represent friction acting on the ith link along x-axis and y-axis respectively. The variables $\varepsilon_{x,i}$ and $\varepsilon_{y,i}$ represent joint constraint forces on link i from link $i+1$ along x-axis and y-axis respectively. The variables $\varepsilon_{x,i-1}$ and $\varepsilon_{y,i-1}$ represent joint constraint forces on link i from link $i-1$ along x-axis and y-axis respectively.

The torque balance equation for the ith link can be written as

$$J\theta_i = u_i - u_{i-1} - l\sin\theta_i(\varepsilon_{x,i} + \varepsilon_{x,i-1}) + l\cos\theta_i(\varepsilon_{y,i} + \varepsilon_{y,i-1}) \tag{84}$$

Suppose the anisotropic viscous friction forces acting on all links are given by

$$\begin{bmatrix} f_x \\ f_y \end{bmatrix} = -\begin{bmatrix} c_t C_\theta^2 + c_n S_\theta^2 & (c_t - c_n)S_\theta C_\theta \\ (c_t - c_n)S_\theta C_\theta & c_t S_\theta^2 + c_n C_\theta^2 \end{bmatrix} \begin{bmatrix} \dot{x} \\ \dot{y} \end{bmatrix} \tag{85}$$

where $S_\theta \in \mathbb{R}^{6\times 6}$ and $C_\theta \in \mathbb{R}^{6\times 6}$ are defined as

$$\begin{aligned} S_\theta &= \mathrm{diag}([\sin(\theta_1), \cdots, \sin(\theta_6)]) \\ C_\theta &= \mathrm{diag}([\cos(\theta_1), \cdots, \cos(\theta_6)]) \end{aligned} \tag{86}$$

Define

$$X = L^T(HH^T)^{-1}H \tag{87}$$

where matrices $L \in \mathbb{R}^{5\times 6}$ and $H \in \mathbb{R}^{5\times 6}$ are in the forms of

$$L = \begin{bmatrix} 1 & 1 & & & & \\ & \cdot & \cdot & & & \\ & & \cdot & \cdot & & \\ & & & 1 & 1 \end{bmatrix} \text{ and } H = \begin{bmatrix} 1 & -1 & & & & \\ & \cdot & \cdot & & & \\ & & \cdot & \cdot & & \\ & & & 1 & -1 \end{bmatrix} \tag{88}$$

Combining (82)-(85) for all six links yields

$$\tilde{M}(\theta)\ddot{\theta} + \tilde{W}(\theta)\dot{\theta}^2 + \tilde{F}(\theta, \dot{\theta}) = H^T u \tag{89}$$

where

$$\begin{aligned} \tilde{M}(\theta) &= JI_n + \tilde{m}l^2(S_\theta V S_\theta + C_\theta V C_\theta) \\ \tilde{W}(\theta) &= \tilde{m}l^2(S_\theta V C_\theta - C_\theta V S_\theta) \\ \tilde{F}(\theta, \dot{\theta}) &= -lS_\theta X f_x + lC_\theta X f_y \end{aligned} \tag{90}$$

In (90) f_x and f_y are defined in (85) and

$$V = L^T(HH^T)^{-1}L \tag{91}$$

To formulate (89) into one with symmetry, a coordinate transformation is defined as

$$\theta = Rq \tag{92}$$

where $R \in \mathbb{R}^{6\times 6}$ is defined as

$$R = \begin{bmatrix} 1 & 1 & 1 & 1 & 1 & 1 \\ 0 & 1 & 1 & 1 & 1 & 1 \\ 0 & 0 & 1 & 1 & 1 & 1 \\ \vdots & & & & & \\ 0 & 0 & 0 & 0 & 0 & 1 \end{bmatrix} \tag{93}$$

and in the new coordinate, (89) can be written as

$$M(q_a)\ddot{q} + W(q)q^2 + F(q,\dot{q}) = Bu \tag{94}$$

where B is defined in (2) and

$$\begin{aligned} M(q_a) &= R^T \tilde{M}(Rq)R \\ W(q)q^2 &= R^T \tilde{W}(Rq)\mathrm{diag}(R\dot{q})R\dot{q} \\ F(q,\dot{q}) &= R^T \tilde{F}(Rq, R\dot{q}) \end{aligned} \tag{95}$$

Notice that (94) has a similar structure as in (1) and therefore the proposed scheme is applicable to (94).

4.1. Simulation results

Here the design and simulation results are presented. The length of a link is chosen to be $l = 0.1m$. The mass of each link is assumed to be $\tilde{m} = 1kg$ and the corresponding moment of inertia is $J = 0.0016kg \cdot m^2$. The friction coefficients are selected as $c_t = 0.5$ and $c_n = 10$. The modulation function defined in (31) is chosen as $K = 1.5$. The modulation function $\mathcal{K}$ and the scalar ϱ defined in (65) is selected as $\mathcal{K} = 20$ and $\varrho = 3$, respectively. In (27), the design freedom Λ is selected as $\Lambda = 5I_4$. During the simulation, the sampling time is chosen to be 0.01 and the solver is chosen as *ode1* for the purpose of simplifying the future implementation.

It is easy to verified from the structure of $M_{22}^{-1}(q_a)$ and $M_{21}(q_a)$ that the vector of one forms $M_{22}^{-1}(q_a)M_{21}(q_a)d_{q_a}$ does not have exact forms. Since there exists one unactuated variable in this example, h can be selected as $h = 1$. Then from (24) it follows $i = j = 1$. Clearly, the left side and the

right side of (23) are equal in the situation when $i = j = 1$, which verifies Assumption 2.4. Since $h = 1$, the virtual control law v_2 is calculated to maintain four actuated variables (i.e. $q_{v2} = [\phi_1, \ \cdots, \ \phi_4]^T$) on the sliding manifolds defined in (27), such that $q_{v2} \to 0$ in finite time. Since during sliding on s, $q_{v2} = 0$, and it can be obtained from (94) that

$$M_{22}(q_{v1}) = \frac{1}{12}\cos(q_{v1}) + \frac{191}{300} \ \text{ and } \ M_{211}(q_{v1}) = \frac{\cos(\phi_5) + 15}{24} \tag{96}$$

and therefore the function $\gamma(q_{v1})$ in (39) is

$$\gamma(q_{v1}) = \int_0^{\phi_5} \frac{25cos(\tau) + 375}{50cos(\tau) + 382} d\tau \tag{97}$$

From (96) and (97), the global change of coordinate in (39) is calculated to transform the reduced order sliding motion to one in a strict feedback norm form where only $q_{v1} = \phi_5$ and $q_u = \theta_6$ are contained.

From the structure of $M_{22}(q_{v1})$ defined in (96), the upper and lower bounds of $M_{22}^{-1}(q_{v1})$ is known and the scalars β_1 and β_2 in Lemma 3.1 can thus be selected as $\beta_1 = 1.38$ and $\beta_2 = 1.58$, respectively. Furthermore, the design parameters Ψ_1 and Ψ_2 defined in (51) are chosen to be $\Psi_1 = 3$ and $\Psi_2 = 30$, respectively, and Lemma 3.1 can then be verified. In this paper the external disturbances are friction associated with the rotational motion of the link, i.e. $d = -c_n J q^2$.

The initial values of q is chosen to be

$$q(0) = [0.35 \quad -0.1 \quad 0.2 \quad -0.7 \quad -0.2 \quad -0.6] \tag{98}$$

The discontinued terms in (31) and (65) are approximated to any level of accuracy using

$$v_{2n} = -K(t)\frac{s}{\|s\| + 0.01} \tag{99}$$

and

$$v_{1n} = -(\frac{\partial g_r}{\partial p_s})^{\dagger}(\mathcal{K}(t)\frac{\Phi}{||\Phi|| + 0.01} + \varrho\Phi) \tag{100}$$

Under anisotropic friction conditions, the friction forces f_x and f_y, acting in the tangential and normal direction of the links, are shown in Fig. 2 and Fig. 3, respectively. It is obvious to see that the friction forces are vanishing due to the regulation process of the joint angles.

The relative joint angles q_{v2}, i.e. ϕ_1, ϕ_2,ϕ_3 and ϕ_4, are shown in Fig. 4. It can be easily seen that they approach to zero in finite time despite non-zero initial relative joint angles and external disturbances. The sliding manifolds s in (27), associated with q_{v2}, are shown in Fig. 5. It is clear from Fig. 5 that the sliding can be induced and maintained afterwards. In Fig. 6, the blue curve represents the heading angle θ_6 and the red curve presents the remaining one actuated variables ϕ_5. It can be seen from Fig. 6 that both ϕ_5 and θ_6 converge to the origin asymptotically despite their non-zero initial values and external disturbances. The sliding manifold Φ in (51) is shown in Fig. 7. The signals v_{1l} and v_{1n}, corresponding to continuous part and discontinuous part of v_1, are shown in Fig. 8 and Fig. 9, respectively. The function $g_r(\cdot)$ in the reduced order system (41) is shown in Fig. 10. Since $g_r(\cdot)$ is a function of ϕ_5, θ_6 and their first order derivatives which approach to zero as shown in Fig. 6, g_r is also vanishing.

Finally, the control inputs u_i for all $i = 1, \cdots, 5$ are shown in Fig. 11. Clearly chattering does not appear in control signals and the required torques or control effect are realistic for the implementation purpose.

Notice that it can be seen from the nonlinear dynamic equation (89) that there always exists a trade-off between the number of the links (i.e. the adaptation level of the system) and the computational load. If the number of the links is large and the computational load estimated from the simulation is not acceptable for the implementation of the control law, we could use the Taylor expansion method to simplify the nonlinear model.

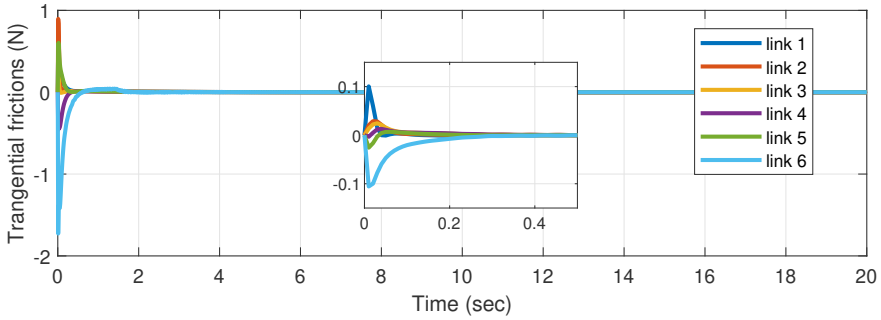

Figure 2: The friction acting in the tangential direction f_x

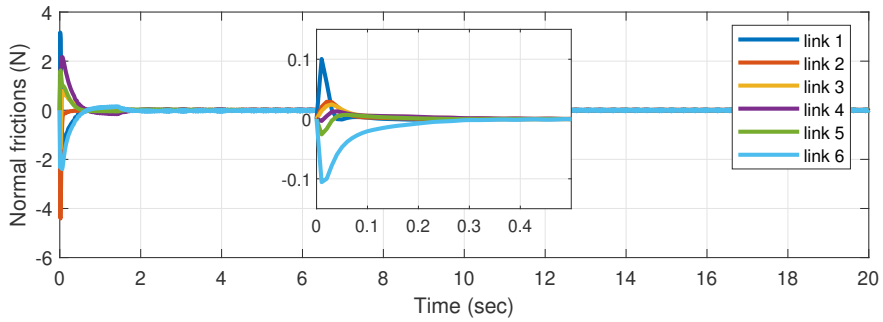

Figure 3: The friction acting in the normal direction f_y

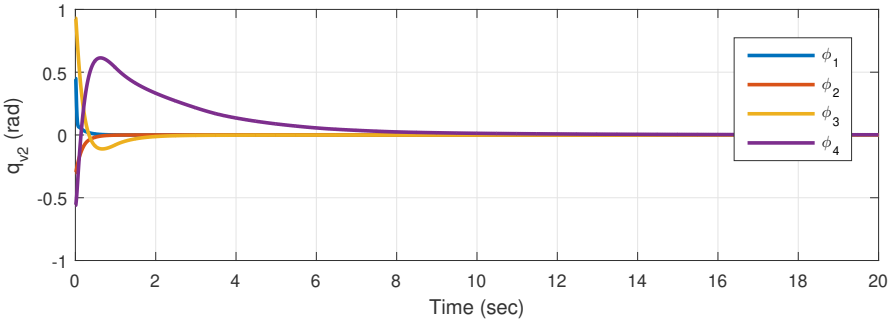

Figure 4: The relative joint angles q_{v2}

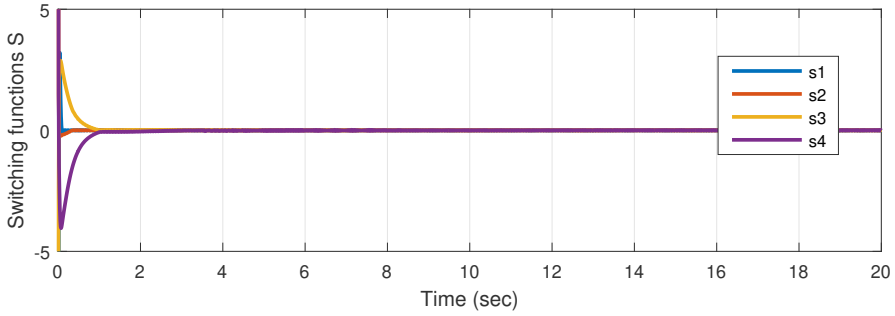

Figure 5: The sliding manifolds s

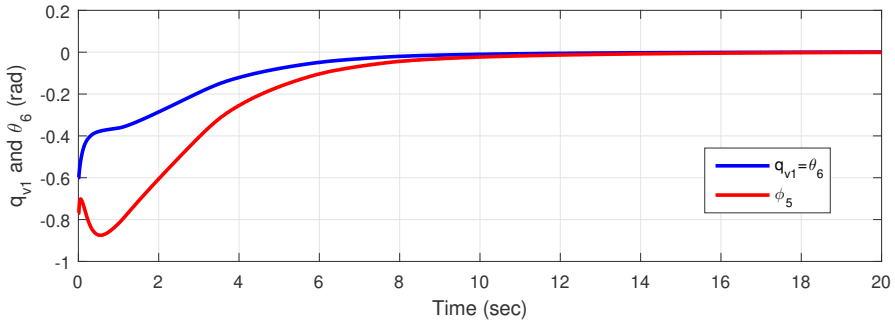

Figure 6: q_{v1} and θ_6

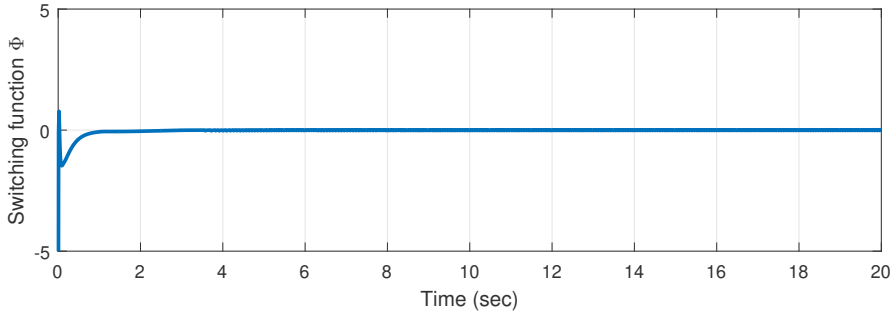

Figure 7: The sliding manifold Φ

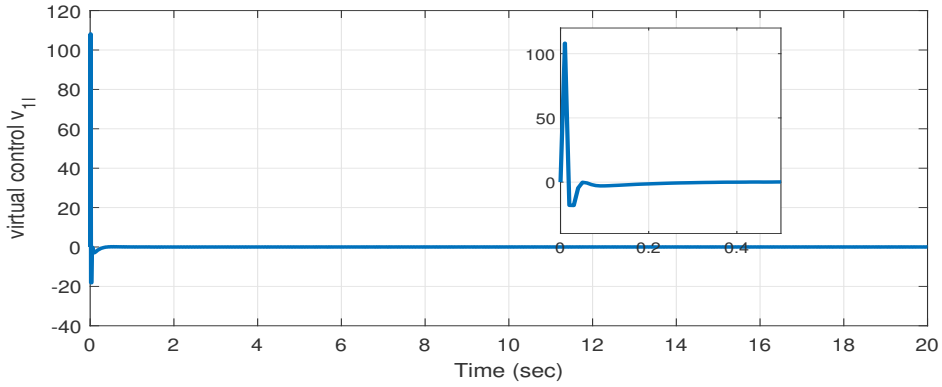

Figure 8: The virtual control v_{1l}

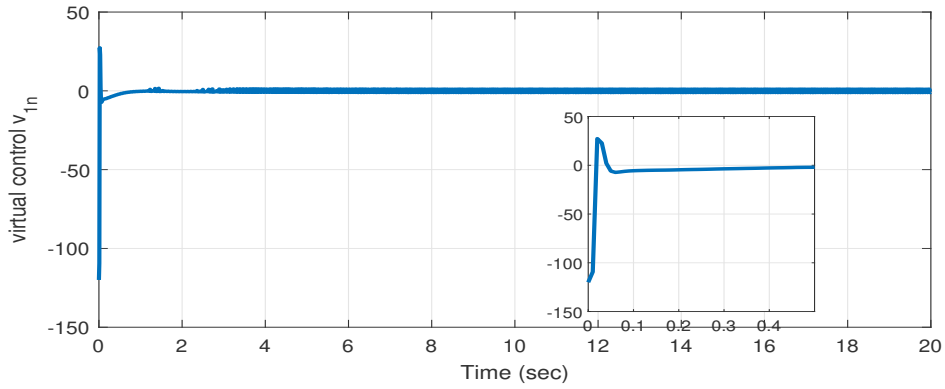

Figure 9: The virtual control v_{1n}

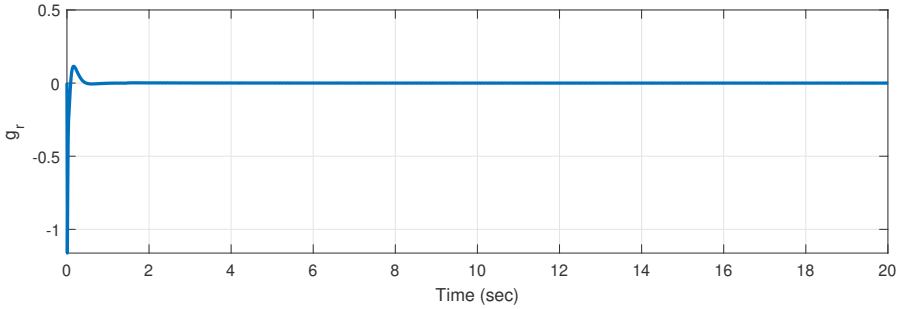

Figure 10: The function g_r

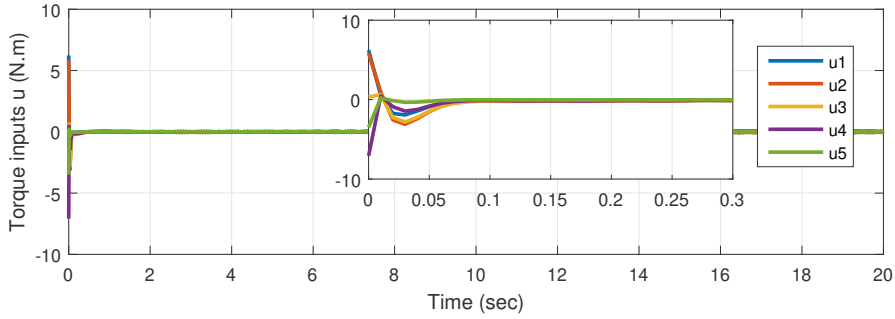

Figure 11: The torque inputs u

5. Conclusion

In this paper, a sliding mode control scheme was developed to stabilise a class of nonlinear perturbed underactuated system with a non-integral momentum. In this scheme, a subset of the actuated variables were initially selected to be maintained on sliding surfaces. During sliding, the system with a non-integrable momentum was approximated by one with an integrable momentum, and a global change of coordinate was found to transform reduced order sliding dynamic into one in the strict feedback normal form. This scheme also contained a sliding mode control law which is derived from the strict feedback form and allows the remaining actuated and unactuated variables to converge to the origin. The design efficacy was verified via a six-link planar robot case study. The future works include: a) a consideration of the situation in which the underactuated systems are not with symmetry; b) the application of the design scheme to the practical multi-link robotic platform.

References

Ashrafiuon, H., & Erwin, R. S. (2008). Sliding mode control of underactuated multibody systems and its application to shape change control. *International Journal of Control*, *81*, 1849–1858.

Chen, T., & Shan, J. (2020). Distributed tracking of a class of underactuated Lagrangian systems with uncertain parameters and actuator faults. *IEEE Transactions on Industrial Electronics*, *67*, 4244–4253.

Cheng, C.-C., & Chen, C.-Y. (1996). Controller design for an overhead crane system with uncretainty. *Control Engineering Practice*, *4*, 645 – 653.

Do, V., & Lee, S. (2020). Neural integral backstepping hierarchical sliding mode control for a ridable ballbot under uncertainties and input saturation. *IEEE Transactions on Systems, Man, and Cybernetics: Systems*, (pp. 1–14).

Dong, Y., & Chen, J. (2019). Adaptive control for rendezvous problem of networked uncertain Euler-Lagrange systems. *IEEE Transactions on Cybernetics*, *49*, 2190–2199.

Du, C., Li, F., & Yang, C. (2020). An improved homogeneous polynomial approach for adaptive sliding-mode control of markov jump systems with actuator faults. *IEEE Transactions on Automatic Control*, *65*, 955–969.

Du, C., Yang, C., Li, F., Gui, W., & Li, W. (2019). Design and implementation of observer-based sliding mode for underactuated rendezvous system. *IEEE Transactions on Systems, Man, and Cybernetics: Systems*, (pp. 1–12).

Edwards, C., & Spurgeon, S. K. (1998). *Sliding Mode Control: Theory and Applications*. London, U.K.: Taylor & Francis.

Fang, Y., Ma, B., Wang, P., & Zhang, X. (2012). A motion planning-based adaptive control method for an underactuated crane system. *IEEE Transactions on Control Systems Technology*, *20*, 241–248.

Ghommam, J., & Mnif, F. (2009). Coordinated path-following control for a group of underactuated surface vessels. *IEEE Transactions on Industrial Electronics*, *56*, 3951–3963.

Hu, C., Wang, R., Yan, F., & Chen, N. (2016). Robust composite nonlinear feedback path-following control for underactuated surface vessels with desired-heading amendment. *IEEE Transactions on Industrial Electronics*, *63*, 6386–6394.

Huang, J., Ri, S., Fukuda, T., & Wang, Y. (2019). A disturbance observer based sliding mode control for a class of underactuated robotic system with mismatched uncertainties. *IEEE Transactions on Automatic Control*, *64*, 2480–2487.

Jiang, S., Zhao, J., Xie, F., Fu, J., Wang, X., & Li, Z. (2018). A novel adaptive sliding mode control for manipulator with external disturbance. In *2018 37th Chinese Control Conference (CCC)* (pp. 3024–3028).

Lai, X., Zhang, P., Wang, Y., & Wu, M. (2017). Position-posture control of a planar four-link underactuated manipulator based on genetic algorithm. *IEEE Transactions on Industrial Electronics*, *64*, 4781–4791.

Li, F., Du, C., Yang, C., Wu, L., & Gui, W. (2019). Finite-time asynchronous sliding mode control for markovian jump systems. *Automatica*, *109*, 108503.

Lu, B., Fang, Y., & Sun, N. (2018a). Continuous sliding mode control strategy for a class of nonlinear underactuated systems. *IEEE Transactions on Automatic Control*, *63*, 3471–3478.

Lu, B., Fang, Y., Sun, N., & Wang, X. (2018b). Antiswing control of offshore boom cranes with ship roll disturbances. *IEEE Transactions on Control Systems Technology*, *26*, 740–747.

Nersesov, S. G., Ashrafiuon, H., & Ghorbanian, P. (2014). On estimation of the domain of attraction for sliding mode control of underactuated nonlinear systems. *International Journal of Robust and Nonlinear Control*, *24*, 811–824.

Olfati-Saber, R. (2000). Cascade normal forms for underactuated mechanical systems. In *Proceedings of the 39th IEEE Conference on Decision and Control (Cat. No.00CH37187)* (pp. 2162–2167). volume 3.

Olfati-Saber, R. (2001). *Nonlinear Control of Underactuated Mechanical Systems with Application to Robotics and Aerospace Vehicles*. Ph.D. thesis MIT.

Olfati-Saber, R. (2002). Normal forms for underactuated mechanical systems with symmetry. *IEEE Transactions on Automatic Control*, *47*, 305–308.

Park, M., Chwa, D., & Hong, S. (2006). Decoupling control of a class of underactuated mechanical systems based on sliding mode control. In *2006 SICE-ICASE International Joint Conference*.

Roy, S., & Baldi, S. (2020). Towards structure-independent stabilization for uncertain underactuated Euler-Lagrange systems. *Automatica*, *113*, 108775.

Shah, I., & Rehman, F. U. (2018). Smooth second order sliding mode control of a class of underactuated mechanical systems. *IEEE Access*, *6*, 7759–7771.

Shoji, T., Katsumata, S., Nakaura, S., & Sampei, M. (2013). Throwing motion control of the springed pendubot. *IEEE Transactions on Control Systems Technology*, *21*, 950–957.

Shtessel, Y., Edwards, C., Fridman, L., & Levant, A. (2013). *Sliding mode control and observation*. Basel: Springer.

Spong, M. W. (1996). Energy based control of a class of underactuated mechanical systems. *IFAC Proceedings Volumes*, *29*, 2828 – 2832.

Spong, M. W., Hutchinson, S., & Vidyasagar, M. (2004). *Robot dynamics and control*. John Wiley & Sons.

Utkin, V. (1992). *Sliding modes in control and optimization*. Springer.

Van, M., Mavrovouniotis, M., & Ge, S. S. (2019). An adaptive backstepping nonsingular fast terminal sliding mode control for robust fault tolerant control of robot manipulators. *IEEE Transactions on Systems, Man, and Cybernetics: Systems*, *49*.

Wang, N., Xie, G., Pan, X., & Su, S. (2019). Full-state regulation control of asymmetric underactuated surface vehicles. *IEEE Transactions on Industrial Electronics*, *66*, 8741–8750.

Wang, Y., Lai, X., Zhang, P., & Wu, M. (2020). Control strategy based on model reduction and online intelligent calculation for planar n -link underactuated manipulators. *IEEE Transactions on Systems, Man, and Cybernetics: Systems*, *50*, 1046–1054.

Wang, Z., Bao, W., & Li, H. (2017). Second-order dynamic sliding-mode control for nonminimum phase underactuated hypersonic vehicles. *IEEE Transactions on Industrial Electronics*, *64*, 3105–3112.

Xu, R., & Özgüner, U. (2008). Sliding mode control of a class of underactuated systems. *Automatica*, *44*, 233 – 241.

Yan, Z., Lai, X., Meng, Q., & Wu, M. (2019). A novel robust control method for motion control of uncertain single-link flexible-joint manipulator. *IEEE Transactions on Systems, Man, and Cybernetics: Systems*, (pp. 1–8).

Zhao, B., Xian, B., Zhang, Y., & Zhang, X. (2015). Nonlinear robust adaptive tracking control of a quadrotor uav via immersion and invariance methodology. *IEEE Transactions on Industrial Electronics*, *62*, 2891–2902.

Zou, Y., & Meng, Z. (2019). Immersion and invariance-based adaptive controller for quadrotor systems. *IEEE Transactions on Systems, Man, and Cybernetics: Systems*, *49*, 2288–2297.